



**HAL**  
open science

## Are low-frequency quasi-periodic oscillations in accretion flows the disk response to jet instability?

Jonathan Ferreira, Grégoire Marcel, Pierre-Olivier Petrucci, Jérôme Rodriguez, Julien Malzac, Renaud Belmont, Maïca Clavel, Gilles Henri, Stéphane Corbel, Mickaël Coriat

### ► To cite this version:

Jonathan Ferreira, Grégoire Marcel, Pierre-Olivier Petrucci, Jérôme Rodriguez, Julien Malzac, et al.. Are low-frequency quasi-periodic oscillations in accretion flows the disk response to jet instability?. *Astronomy and Astrophysics - A&A*, 2022, 660, pp.A66. 10.1051/0004-6361/202040165 . hal-03640831

**HAL Id: hal-03640831**

**<https://hal.science/hal-03640831v1>**

Submitted on 13 Apr 2022







**HAL** is a multi-disciplinary open access archive for the deposit and dissemination of scientific research documents, whether they are published or not. The documents may come from teaching and research institutions in France or abroad, or from public or private research centers.

L'archive ouverte pluridisciplinaire **HAL**, est destinée au dépôt et à la diffusion de documents scientifiques de niveau recherche, publiés ou non, émanant des établissements d'enseignement et de recherche français ou étrangers, des laboratoires publics ou privés.



Distributed under a Creative Commons Attribution 4.0 International License

# Are low-frequency quasi-periodic oscillations in accretion flows the disk response to jet instability?

J. Ferreira<sup>1</sup>, G. Marcel<sup>2</sup>, P.-O. Petrucci<sup>1</sup>, J. Rodriguez<sup>3</sup>, J. Malzac<sup>4</sup>, R. Belmont<sup>3</sup>, M. Clavel<sup>1</sup>, G. Henri<sup>1</sup>, S. Corbel<sup>3</sup>, and M. Coriat<sup>4</sup>

<sup>1</sup> Univ. Grenoble Alpes, CNRS, IPAG, 38000 Grenoble, France  
e-mail: [jonathan.ferreira@univ-grenoble-alpes.fr](mailto:jonathan.ferreira@univ-grenoble-alpes.fr)

<sup>2</sup> Institute of Astronomy, University of Cambridge, Madingley Road, Cambridge CB3 0HA, UK

<sup>3</sup> AIM, CEA, CNRS, Université Paris-Saclay, Université de Paris, 91191 Gif-sur-Yvette, France

<sup>4</sup> IRAP, Université de Toulouse, CNRS, UPS, CNES, Toulouse, France

Received 18 December 2020 / Accepted 30 January 2022

## ABSTRACT

Low-frequency quasi-periodic oscillations, or LFQPOs, are ubiquitous in black hole X-ray binaries and provide strong constraints on the accretion-ejection processes. Although several models have been proposed, none has been proven to reproduce all observational constraints, and no consensus has emerged so far. We make the conjecture that disks in binaries are threaded by a large-scale vertical magnetic field that splits it into two radial zones. In the inner jet-emitting disk (JED), a near equipartition field allows driving powerful self-collimated jets, while beyond a transition radius, the disk magnetization is too low and a standard accretion disk (SAD) is settled. In a series of papers, this hybrid JED-SAD disk configuration has been shown to successfully reproduce most multiwavelength (radio and X-rays) observations, as well as the concurrence with the LFQPOs for the archetypal source GX 339-4. We first analyze the main QPO scenarios provided in the literature: (1) a specific process occurring at the transition radius, (2) the accretion-ejection instability, and (3) the solid-body Lense-Thirring disk precession. We recall their main assumptions and shed light on some severe theoretical issues that question the capability of reproducing LFQPOs. We then argue that none of these models can be operating under JED-SAD physical conditions. We finally propose an alternative scenario according to which LFQPOs are the disk response to an instability triggered in the jets near a magnetic recollimation zone. This situation can account for most of the type C QPO phenomenology and is consistent with the global behavior of black hole binaries. This nondestructive jet instability remains to be calculated, however. If this instability is numerically confirmed, then it might also naturally account for the jet wobbling phenomenology seen in various accreting sources such as compact objects and young forming stars.

**Key words.** ISM: jets and outflows – accretion, accretion disks – magnetohydrodynamics (MHD) – galaxies: active – X-rays: binaries

## 1. Introduction

Black hole X-ray binaries (hereafter XrB) are binary systems in which a stellar-mass black hole accretes matter from a low-mass companion star. The incoming mass forms an accretion disk around the black hole that is mainly detected in X-rays. All systems are X-ray transients, which sometimes spend years in a barely detectable quiescence and suddenly increase their luminosity by factors up to  $10^6$  for some months, until they return to quiescence (see, e.g., [Remillard & McClintock 2006](#); [Done et al. 2007](#); [Dunn et al. 2010](#)). These episodes of intense activity are accompanied by drastic spectral changes, with two main canonical spectral states. In the hard state, the spectrum is dominated by a (cutoff) power-law-like emission that is usually attributed to inverse Comptonization that peaks at a few 100 keV and shows a quite intense (10–20% rms) rapid (subsecond) variability. In the soft state, the spectrum is characterized by thermal blackbody emission of a few keV only and exhibits much less variability. A complete outburst cycle can then be followed in a hardness-intensity diagram (HID), where most black hole sources create a *q*-shaped evolutionary track (see, e.g., [Dunn et al. 2010](#)). Starting at low emission and in the hard state, an outburst consists first of a tremendous increase in luminosity in the hard state, a sharp transition to a softer (low hardness) state

while maintaining a roughly constant luminosity, followed by a luminosity decrease while remaining in this soft state, another transition back to the hard state at roughly the same luminosity, and a final decay back to the initial state (completing the *q*-shape).

The HID only probes accretion onto the black hole, however, and does not convey the entire phenomenology of these sources. It is now well known that jets, possibly in the form of bipolar self-confined outflows, are also emitted by the central regions. These jets are mainly detected in radio bands and show a clear correlation with the underlying X-ray emission, but only when the source is in the hard state (see, e.g., [Corbel et al. 2000, 2003, 2013](#); [Gallo et al. 2003](#); [Merloni et al. 2003](#); [Falcke et al. 2004](#); [Fender et al. 2004](#) and the review by [Fender & Gallo 2014](#)). While explaining the behavior seen in the HID alone was already quite challenging per se, including the jet production mechanism (and its associated power leakage in the hard states) remains an open issue. Several propositions have been made (e.g., [Esin et al. 1997](#); [Meyer-Hofmeister et al. 2005](#); [Yuan et al. 2005](#); [Ferreira et al. 2006b](#); [Begelman & Armitage 2014](#); [Kylafis & Belloni 2015](#)), but to date, there is no clear consensus about the scenario that is most likely to explain the complex multiwavelength (radio to X-rays) time-dependent behavior of black hole XrBs.

The analysis of the fast timing variations seen in hard X-rays offers another independent means of grasping the black hole XRBs phenomenology, however (see [Motta 2016](#); [Ingram & Motta 2019](#) for recent reviews). The intrinsic variability of the sources is highly dependent on their spectral state and reaches 20% in the hard states, decreases to 1–10% level in the hard-to-soft and soft-to-hard intermediate states, and is often consistent with zero in the soft state. In addition, the power density spectra have complex and state-dependent shapes. On top of a broad band continuum, they can exhibit narrow features, called quasi-periodic oscillations or QPOs, of centroid frequency  $\nu$  and extent  $\Delta\nu$ . There are three main types of low-frequency ( $\nu < 50$  Hz) QPOs that seem intimately linked to the spectral state ([Remillard et al. 1999](#); [Casella et al. 2004](#); [Belloni et al. 2005](#)): type C, the most common, are detected in hard states, type B appear during (and define) the intermediate states, and type A are rare and are only seen in the high-soft state. Type A QPOs are very weak and broad with  $Q = \nu/\Delta\nu < 3$  and a frequency  $\nu_A \sim 6$ –8 Hz. Type B QPOs are more prominent and narrow, with  $Q \geq 6$  and  $\nu_B \sim 1$ –6 Hz. Finally, type C QPOs are strong and narrow, with  $Q \geq 10$  and a frequency  $\nu_C$  ranging from mHz to  $\sim 10$  Hz.

Although there is a time sequence from one QPO type to the next, it is unclear whether all types can be explained by the same model. For instance, type B QPOs are stronger in more face-on objects and reveal a time proximity with transient radio flares, which has led to the proposition of a link between their appearance and the launching of discrete relativistic ejections ([Fender et al. 2009](#); [Motta et al. 2015](#); [Stevens & Uttley 2016](#); [Russell et al. 2019](#); [Homan et al. 2020](#)). These two properties are not shared by all QPOs, however. Type A QPOs are detected in a jetless phase, while type C QPOs are characterized by three additional properties ([Remillard & McClintock 2006](#); [Motta 2016](#)). First, the frequency  $\nu_C$  is independent of the energy band and source inclination, although it is always associated with the inner (hot) accretion flow (e.g., [van den Eijnden et al. 2017](#)). Second, the time evolution of the QPO frequency is tightly correlated with the variation in the soft ( $< 10$  keV) source count rate and hard X-ray power-law index, as well as with the innermost radius of the cold (blackbody) accretion flow. However, the QPO frequencies are always much lower than the Keplerian frequency of the inner cold disk radius (e.g., [Muno et al. 1999](#); [Markwardt et al. 1999](#); [Sobczak et al. 2000](#); [Rodriguez et al. 2002, 2004b](#); [Vignarca et al. 2003](#); [Remillard & McClintock 2006](#); [Marcel et al. 2020](#)). Finally, phase lags are also commonly observed between different energy bands (e.g., 2–5 versus 13–30 keV; [Casella et al. 2004](#)). The lag of a type C QPO is strongly correlated with its frequency and also depends on the object inclination: near zero, but with an increasing hard lag (soft photons arriving first) with increasing QPO frequency for low-inclination sources, whereas high-inclination sources turn to soft lags at higher QPO frequencies (e.g., [Motta et al. 2015](#); [van den Eijnden et al. 2017](#); [de Ruiter et al. 2019](#); [Zhang et al. 2020](#); [Ma et al. 2021](#)).

Explaining type C LFQPOs is a challenging task, and several models have been proposed in the literature. No consensus has been reached so far, however, because all QPO models still face major theoretical issues. Moreover, and more importantly, no model embraces the global picture of these accreting systems. As intriguing as QPOs may be, they are only an epiphenomenon of the main accretion-ejection process. They must therefore be understood within, and be part of, a global framework that also addresses the other observational constraints, that is, spectral evolution, jet formation, and quenching.

Hereafter, we focus on such a framework, the hybrid disk configuration proposed by [Ferreira et al. \(2006b\)](#), which has recently been successfully compared to observations in a series of papers ([Marcel et al. 2018a,b, 2019, 2020, 2022](#); [Ursini et al. 2020](#); [Marino et al. 2021](#); [Barnier et al. 2022](#)). In this framework, a large-scale vertical magnetic field  $B_z$  is assumed to thread the inner disk regions, for instance, below  $10^4 r_g$ , where  $r_g = GM/c^2$  is the gravitational radius. At any given radius, its dynamical importance is measured at the disk midplane by the magnetization  $\mu(r) = B_z^2/(\mu_o P_{\text{tot}})$ , where  $P_{\text{tot}}$  is the sum of the gas and radiation pressure. It has been argued that this magnetization is a decreasing function of the radius and that the disk is separated into two distinct regions ([Ferreira et al. 2006b](#); [Petrucci et al. 2008](#)). Beyond a transition radius  $r_J$ , the magnetization is low and the disk is assumed to be in a standard accretion disk mode (hereafter SAD, [Shakura & Sunyaev 1973](#)), where most of the disk angular momentum is carried radially away by a turbulence driven by the magneto-rotational instability (hereafter MRI, [Balbus & Hawley 1991](#); [Balbus 2003](#)). Although winds are possible and even expected when a large-scale  $B_z$  field is present, their influence on the disk energetics is rather small ([Zhu & Stone 2018](#); [Jacquemin-Ide et al. 2021](#)). As a consequence, the SAD region accretes at a highly subsonic speed and is optically thick. In contrast, the region below  $r_J$  that extends to the innermost stable circular orbit  $r_{\text{ISCO}}$  is in a jet-emitting disk (hereafter JED) mode, where a sizable fraction of the disk angular momentum is carried away vertically by two self-confined magnetically driven jets. The JED model is a generalization and an extension of the [Blandford & Payne \(1982\)](#) jet model, addressing both the mass-loading issue and causal connection with the underlying disk. This inner JED region is characterized by a magnetic field near equipartition (a constant  $\mu$  around 0.1–0.8), leading to a supersonic accretion speed ([Ferreira & Pelletier 1995](#); [Ferreira 1997](#)). As a consequence, the JED region is much less dense than the outer SAD and becomes optically thin and geometrically slim.

As estimated in [Marcel et al. \(2018a\)](#), radial JED-SAD transition is achieved when the inner disk magnetization in the SAD reaches a value  $\mu_c \sim 10^{-3}$ . This critical value triggers the inward radial transition to a JED and leads to a sudden drop in density and increase in accretion speed as the jet torque becomes dominant. Postulated in 2006, this radial JED-SAD disk configuration seems to be qualitatively consistent with current 3D global MHD simulations, both in nonrelativistic ([Jacquemin-Ide et al. 2021](#)) and relativistic regimes ([Igumenshchev et al. 2003](#); [Tchekhovskoy et al. 2011](#); [McKinney et al. 2012](#); [Avara et al. 2016](#); [Liska et al. 2020](#) to cite only a few). In GRMHD simulations, this inner zone has usually been called magnetically arrested disk or MAD. This model was initially defined as  $B_z B_r^+/\mu_o \sim \rho \Omega_K^2 r h$ , that is, where the poloidal laminar magnetic field would be so strong that it would provide support against gravity. Assuming  $B_r^+ \sim B_z$ , this requires a disk magnetization  $\mu \sim r/h$  (see [Narayan et al. 2003](#) and references therein). On the other hand, a JED is a sub-Keplerian disk with  $\mu$  on the order of unity, which is enough to launch centrifugally driven jets. More numerical efforts must be made to assess the differences between a JED and a MAD.

The JED-SAD framework allows us to reproduce most of the available data for the archetypical source GX 339-4. By allowing the disk accretion rate  $\dot{m}$  and the transition radius  $r_J$  to vary independently with time, four activity cycles have been successfully reproduced (see [Marcel et al. 2020](#) and references therein). It is remarkable that time evolutions of the pair  $(r_J, \dot{m})$  are able to reproduce each individual spectrum and the HID of GX 339-4,

but also the radio emission (although in a more qualitative way). Moreover, it has been firmly established that the frequency of the detected Type-C LFQPOs follows the scaling law

$$\nu_{\text{QPO}} = \nu_K(r_J)/\chi, \quad (1)$$

where  $\nu_K(r_J)$  is the Keplerian orbital frequency at  $r_J$ , and  $\chi$  is a constant factor  $\sim 100$  (which varies from 70 to 130, depending on the outburst cycle). This result, verified for more than two decades in frequencies, clearly advocates for a strong connection between the physical source of the LFQPO and the transition radius  $r_J$  (Marcel et al. 2020).

To our knowledge, and despite several simplifications, this framework is currently the only one providing a clear picture that addresses most of the observational accretion-ejection constraints. However, it is unclear whether the observed timing properties, and in particular the LFQPOs, can fit inside this paradigm. Answering this question is the purpose of this paper.

We first critically analyze in Sect. 2 the main QPO scenarios provided in the literature: a specific process triggered at the transition radius, the accretion-ejection instability (Tagger & Pellat 1999), and solid-body Lense-Thirring disk precession model (Ingram et al. 2009). We recall their main results, but also highlight (sometimes severe) theoretical issues (see Ingram & Motta 2019; Marcel & Neilsen 2021 for observational issues). Regardless of these issues, we argue moreover that none of these scenarios can explain type C QPOs that fulfill Eq. (1) within the JED-SAD framework. In Sect. 3 we finally propose a novel scenario in which the observed LFQPOs would be the inner JED response to a jet instability occurring away from the disk. We show in Sect. 4 that this situation not only provides a qualitative explanation for the LFQPO phenomenology, but may also provide insights into the behavior of astrophysical jets. We conclude in Sect. 5.

## 2. Comments on some models for LFQPOs

Before proposing a new scenario for the LFQPO (Sect. 3), we first discuss several existing models in this section. We only address those that in our view are the most representative in the literature and refer to the reviews of Done et al. (2007) and Ingram & Motta (2019) for an exhaustive list. All models require a transition radius that usually is associated with the innermost blackbody disk. When applicable, we also discuss some of these models in the context of the JED-SAD framework.

### 2.1. Specific process occurring at the transition radius

Because the QPO frequency in hard X-ray emission is tightly correlated with the transition radius (labeled  $r_J$  in the JED-SAD framework), it is natural to first examine a physical process that would be triggered at that specific location. The problem is the factor  $\chi \sim 100$ , which requires searching for a very slow, secular process.

It is known, for instance, that any misalignment between the black hole spin and the disk leads to a Lense-Thirring (hereafter LT) precession due to the dragging of inertial frames (see Bardeen & Petterson 1975 and references therein). As a consequence, a test particle located at a radius  $r$  from a black hole of dimensionless angular momentum  $j$  would undergo a relativistic precession at the LT-frequency  $\nu_{\text{LT}}(r) \simeq \frac{jc}{\pi r_g} (r/r_g)^{-3}$ , which steeply decreases with the distance. Proposed initially for kHz QPOs in XrBs (Stella & Vietri 1998; Stella et al. 1999), the outskirts of a hot inner flow, specifically, a hot ring near the tran-

sition radius with the SAD, might equally be thought to provide an observable LFQPO. However, the ratio  $\nu_{\text{LT}}/\nu_K(r_J) = 2j(r_J/r_g)^{-3/2} \propto r_J^{-3/2}$  continues to decrease with the distance. This contradicts the observational constraint Eq. (1), where this ratio remains roughly constant regardless of  $r_J$ .

Motivated by the similarity between the observed power-density spectra of black hole XrBs and the response function to external perturbations of driven mechanical and electrical systems, Psaltis & Norman (2000) computed the response of a narrow (of  $\delta r/r \sim 0.01$ ), geometrically thin accretion disk annulus to a broad spectrum of isothermal perturbations imposed outside of it. This ring corresponds to an abrupt change in disk properties, probably again the transition radius. They found that some resonances appear to be superimposed on the incoming spectrum, leading to observable QPOs. Because they neglected the radial pressure forces, the predicted mode frequencies mostly depend on the gravitational field around the compact object and only weakly on the hydrodynamic properties of the flow itself. As a result, the selected frequencies are related to the epicyclic and LT frequencies at the transition radius, neither of which can explain LFQPOs due to the huge factor  $\chi$ .

Kato & Manmoto (2000) proposed a model of trapped oscillations that would be triggered at the transition radius between the outer SAD and an inner advection-dominated accretion flow, or ADAF (Ichimaru 1977; Narayan & Yi 1994, see also the review by Yuan & Narayan 2014). This situation implies a very narrow transition zone in which the rotation profile needs to become slightly super-Keplerian (Abramowicz et al. 1998). As a consequence, the epicyclic frequency  $\kappa^2$  becomes negative, leading to a local instability (Rayleigh criterion, when the stabilizing effects due to the strong inhomogeneities are negligible). The authors then argued that the slowly growing amplitude of the perturbations would remain trapped around the transition radius, leading to local QPOs.

Assuming a particular radial profile for the disk temperature within the transition region, the authors solved the local dispersion relation of these inertial-acoustic modes. They showed that it is possible to fine-tune this radial profile so that the eigenvalue matches the QPO frequency at a given transition radius. However, and this is quite uncomfortable, this fine-tuning must be performed for every radius and for a given set of disk parameters. It therefore seems difficult to reconcile this result with the generic behavior deduced from observations<sup>1</sup>. Not only is there no reason for this fine-tuning to occur, but the model also relies on strong approximations. The neglect of the accretion motion is particularly important. It would unavoidably lower the local growth of perturbations by advecting them.

This remark is even more critical within the JED-SAD framework, which assumes the presence of a large-scale  $B_z$  field everywhere. Whether this instability would be present near  $r_J$  in this case requires a novel investigation. However, the disk material undergoes a transsonic transition at  $r_J$  (Ferreira et al. 2006b; Marcel et al. 2018a; Scepi et al. 2019) because the SAD accretes at subsonic speeds, whereas the JED is supersonic. Moreover, in order for a JED to maintain a constant disk magnetization  $\mu$ , any additional magnetic flux that would be carried in by the accreting flow must be expelled. This is exactly what happens in some GRMHD simulations, where a magnetic Rayleigh-Taylor instability is seen to grow and expel the magnetic flux excess as magnetic bubbles (McKinney et al. 2012;

<sup>1</sup> This fine-tuning is independent of the so-called p-disk model, which is a multi-blackbody disk model in which the temperature exponent is left free (Mineshige et al. 1994; Kubota et al. 2005).



Marshall et al. 2018). Quite interestingly, this is done quasi-periodically but on a timescale comparable to a few Keplerian orbits at  $r_j$ ; this is inconsistent with LFQPOs. The existence of this messy, transsonic JED-SAD transition therefore casts serious doubt on the possibility of allowing the development of any secular instability at that location.

## 2.2. Accretion-ejection instability

The accretion-ejection instability (AEI) has first been studied by Tagger & Pellat (1999) in the context of accretion disks threaded by a large-scale  $B_z$  field and was then proposed to explain QPOs by Varnière et al. (2002) and Rodríguez et al. (2002). A non-axisymmetric ideal MHD instability is found to be triggered whenever the vertical field reaches equipartition along with some radial profile. These spiral waves travel back and forth between the disk inner radius  $r_{in}$  (initially assumed to be the innermost SAD radius) and some radius  $r_{co}$ , defined as the corotation between the wave phase speed and the disk material rotation. The waves transport angular momentum outward, allowing the cavity between  $r_{in}$  and  $r_{co}$  to accrete rapidly. Although spiral waves are also emitted beyond  $r_{co}$ , accretion in this outer region is nevertheless assumed to continue thanks to the usual MRI-driven turbulence. At the corotation radius, waves are evanescent, but a resonance with a vertical Alfvén wave allows the transfer of some energy and angular momentum in the vertical direction. A magnetized azimuthally localized vortex is thus expected to grow at  $r_{co}$ , opening the possibility for some ejection there (but this has not been demonstrated yet). This vortex is invoked to be the locus of enhanced dissipation (a hot spot), leading to a QPO with a frequency  $\nu_K(r_{co})$ , as long as some geometrical occultation is present as well (so that QPOs can only be seen in high-inclination sources).

At first sight, the AEI would perfectly fit at the interface between the JED and SAD zones because of the build-up of a large-scale  $B_z$  field near equipartition in the JED. For the AEI to reproduce the LFQPO behavior encapsulated in Eq. (1), however, the ratio of the corotation radius to the innermost disk radius (equal to  $r_j$  within the JED-SAD framework) must then be  $\chi^{2/3} \gg 1$  (independent of  $r_j$ ). This distance between the inner boundary and the corotation radius cannot be achieved within the AEI framework (see, e.g., Fig. 4 in Varnière et al. 2002). With increasing magnetization, the wavelength increases as well, widens the cavity, and pushes the corotation radius farther out. This also leads to a widening of the forbidden zone around the corotation radius, however, and the amplification mechanism becomes less efficient. As a result, the growth rate has a maximum for  $\mu$  only close to 1 (Tagger & Pellat 1999). In other words, the factor  $\chi \sim 100$  for type C QPOs cannot be achieved within the AEI framework for reasonable values of the magnetic field.

It must also be realized that the complex situation invoked for the AEI has been computed with a highly simplified setup so far. For instance, the toroidal component of the magnetic field has been neglected, which forbids the launching of jets and winds that would seriously affect the disk angular momentum transport. The unavoidable MRI-driven turbulence has also been discarded, while it provides both another torque and wave dissipation, two ingredients that would again lower the efficiency of the mechanism. On the other hand, despite the assumption of a perfect wave reflection at the inner disk boundary, the maximum AEI growth rate is already quite low, namely on the order of only  $V_A/r \sim \mu^{1/2} \Omega_K h/r$  (Tagger & Pellat 1999). This means that the physical ingredients listed above (jets, turbulence) would

probably seriously decrease it or even quench the instability. Finally, the probable presence of a magnetic Rayleigh-Taylor instability at the edge of the JED, as seen in MAD simulations (McKinney et al. 2012; Marshall et al. 2018), questions the very existence of the AEI at that location. Because of all these additional ingredients, assuming a perfectly reflecting boundary at  $r_j$  appears rather dubious indeed.

Because of all these difficulties, and in particular, because of the unreachable factor  $\chi$ , AEI is probably not the source of type C QPOs within the JED-SAD framework. However, for type A and/or type B LFQPOs, which are observed only when  $r_j$  is near the ISCO and when relativistic effects are strong (see Varnière et al. 2012 and references therein), the AEI may remain a possible candidate.

## 2.3. Solid-body Lense-Thirring disk precession model

The solid-body precession of the inner disk due to the Lense-Thirring effect is certainly the most popular model invoked to explain type C LFQPOs (Ingram et al. 2009; Ingram & Motta 2019). This model relies on a geometrical general relativity effect that occurs whenever the black hole spin is misaligned with the disk axis. The resulting frame drag causes strong structural changes in the surrounding accretion disk (precession) as it struggles to adapt its equatorial plane to the periodic changes in the local gravitational field. The model of Ingram et al. (2009) for QPOs has been designed within the framework of Esin et al. (1997): an inner hot, optically thin, and geometrically thick flow (ADAF) is settled until a transition radius  $r_t$  beyond which the disk becomes the usual cold, optically thick, and geometrically thin SAD. Within this framework, a LFQPO correlated with  $r_t$  (hence also with the disk blackbody) could arise if the inner geometrically thick disk (ADAF) modulates the X-ray flux. This can only occur, however, if a significant portion of the ADAF volume is precessing as a solid body, namely with a unique precession frequency  $\nu_{prec}$ .

As shown by Ingram et al. (2009), if this volume extends to the innermost stable orbit, not only would the precession frequency  $\nu_{prec}$  exhibit a too strong dependence on the black hole spin, but it would also provide frequencies that are far too high. As a consequence, it is commonly assumed that the innermost disk regions, up to a few  $r_g$ , are aligned with the black hole spin that is probably due to a Bardeen-Petterson effect (Bardeen & Petterson 1975; Papaloizou & Lin 1995; Lubow et al. 2002). Alignment of the inner zone is always seen in all numerical simulations of tilted black holes (see, e.g., Fragile et al. 2007; Fragile 2009), although the presence of large-scale magnetic fields seems to seriously modify the estimate of this inner radius and even question the physical mechanism (McKinney et al. 2013; Krolik & Hawley 2015; Liska et al. 2018, 2019, 2021; Chatterjee et al. 2020). Nevertheless, assuming an inner radius of a few  $r_g$  and a solid-body LT-precession up to an arbitrary transition radius  $r_t$ , Ingram et al. (2009) have shown that the precession frequency  $\nu_{prec}(r_t)$  could indeed cover the observed frequency range of type C QPOs from  $\sim 0.01$  to  $\sim 10$  Hz. The actual value of  $\nu_{prec}$  is a direct function of the external radius  $r_t$ , which remained a free parameter in this work. Several other observational features related to QPOs have been obtained within this framework (see the review of Ingram & Motta 2019).

However, as appealing as this scenario is, the proof that a solid-body LT-precession is settled over a significant radial range remains controversial in numerical GR simulations. While solid-body precession has clearly been shown in

hydrodynamical flows (see, e.g., [Fragile & Anninos 2005](#); [Dyda & Reynolds 2020](#)), the trend is much less clear when magnetized flows are considered. It has been claimed that there is indeed a volume that undergoes solid-body LT-precession (e.g., [Fragile et al. 2007](#); [Liska et al. 2018, 2019](#)), but no evidence of this has been found in other works (e.g., [McKinney et al. 2013](#); [Sorathia et al. 2013](#); [Krolik & Hawley 2015](#); [Chatterjee et al. 2020](#)). The main reason of this discrepancy is probably the difference in the large-scale magnetic field that accumulates in the central disk regions (i.e., the value of the achieved disk magnetization  $\mu$ ). A vertical field not only triggers an MRI-driven turbulence, but also launches jets from the disk. It is also well known that both effects, turbulence and jets, produce additional torques that may prevent the enforcement of solid-body precession by the Lense-Thirring torque ([Sorathia et al. 2013](#); [McKinney et al. 2013](#)). It is also possible that high tilts ( $65^\circ$ ) would be able to tear off the inner disk up to a radius  $r_t$  and enforce a solid-body precession ([Liska et al. 2021](#)). However, it would be a rather strong implication of the model if, in order to reproduce LFQPOs, high tilts were always required.

In any case, we would like to stress that providing the proof that a significant portion of the disk, for instance, from  $\sim 5r_g$  to  $r_{\text{out}} \sim 20$  or even up to  $100r_g$ , is actually precessing as a solid body is a formidable numerical task. It would require showing, for example, that the local precession angle is the same for the whole range of radii, and that it evolves linearly in time such that  $P(t) - P(0) = \dot{P}t$ , with  $\dot{P} = 2\pi\nu_{\text{QPO}}$ , allowing measuring the QPO frequency (see, e.g., Fig 2 in [Dyda & Reynolds 2020](#)). This requires that disk conditions at  $r_{\text{out}}$  (i.e., accretion rate) are maintained rather constant for a duration  $\Delta T$  that must at the very least be three or four times the QPO period, however, namely  $\Delta T \sim 1-3(r_{\text{out}}/r_g)^{3/2}10^3r_g/c$ . For instance, a 0.1 Hz QPO would require a converged simulation that would last for a few times  $10^5r_g/c$  for a black hole with 10 solar masses. While such long times have recently been achieved in a few simulations (e.g., [Chatterjee et al. 2020](#); [Liska et al. 2021](#)), constant disk conditions in the outer regions are still not met (to our knowledge). This situation is due to the initial conditions, which do not include a steady outer accretion disk. It is therefore very difficult to assess whether solid-body LT-precession has settled in, and this clearly deserves further numerical simulations that are long enough and tailored to maintain an outer cold thin disk.

Notwithstanding these current difficulties, this scenario might fit within our JED-SAD framework. It requires the black hole spin to be misaligned with the disk angular momentum vector, and there is no reason why it should not be (although large tilts are not expected to always be the rule). As a result of the LT-torque, the innermost disk region (up to a few  $r_g$  according to GRMHD simulations) should always be aligned with the black hole spin, regardless of whether the disk is in a JED or in a SAD accretion mode (this alignment may be modified from the usual Bardeen-Petterson mechanism by the presence of large-scale magnetic fields; [Liska et al. 2019, 2021](#)). The question then is what occurs beyond this innermost aligned region, when an inner JED is settled up to a large  $r_J$ .

According to [McKinney et al. \(2013\)](#) and references therein, this question can be answered by comparing the LT-torque with the other local torques acting on the disk. The local LT torque acting on a disk annulus can be estimated as  $\Gamma_{\text{LT}} = \Omega_{\text{LT}}L \sin\beta$ , where  $\Omega_{\text{LT}}$  is the LT-precession pulsation,  $L = \Sigma\Omega_K r^2$  is the disk angular momentum per unit area, and  $\beta$  is the black hole tilt angle (see, e.g., [McKinney et al. 2013](#) and references therein). In a JED, the dominant torque is the magnetic braking provided

by the two jets, and it reads  $\Gamma_{\text{jets}} = -2r \frac{B_\phi^+ B_z}{\mu_0}$ , which leads to a ratio

$$\frac{\Gamma_{\text{LT}}}{\Gamma_{\text{jets}}} = \sin\beta \frac{2j}{q\mu} \frac{r}{h} \left(\frac{r}{r_g}\right)^{-3/2}. \quad (2)$$

In this expression,  $q = -B_\phi^+/B_z$  is the magnetic shear measured at the disk surface,  $\mu$  is the disk magnetization measured at the disk midplane (this does not include turbulent fields), and  $h/r$  is the local disk aspect ratio. Because a hot JED verifies  $q\mu \sim 1$  and  $h/r \sim 0.1$  ([Marcel et al. 2018b](#)), this expression shows that the LT torque is never expected to be dominant in a JED beyond a few  $r_g$ . This conclusion stems only from our assumption that a near equipartition laminar magnetic field exists.

This result can also be understood in other terms. In order for a solid-body LT-precession to take place, the disk must behave as a whole entity. This situation requires that a strong causal connection is maintained between its two radial boundaries. Namely, that bending waves can propagate back and forth and enforce the same precession rate over the entire volume. This wave-like regime has been estimated in hydrodynamical situations to require  $\alpha_v < h/r$ , that is, a turbulent Shakura-Sunyaev  $\alpha_v$  parameter smaller than the disk aspect ratio ([Papaloizou & Lin 1995](#); [Lubow et al. 2002](#)). Because MRI provides a scaling  $\alpha_v \sim 10\mu^{1/2}$  ([Salvesen et al. 2016](#)), this shows that weakly magnetized ( $\mu < 10^{-4}$ ), hot ( $h/r > 0.2$ ) flows might exist in this regime and might indeed undergo solid-body LT-precession. This situation was initially envisioned (with an ADAF as the hot inner flow) and may have been achieved in some weakly magnetized GRMHD numerical simulations. A JED has a near equipartition field ( $\mu \sim 1$ ), however, and accretes at supersonic speeds due to its dominant jet torque. This challenges any upstream wave propagation and certainly thereby forbids the establishment of solid-body LT-precession over its entire volume.

The JED thermal balance calculations performed by [Marcel et al. \(2018a\)](#) led to a disk aspect ratio  $h/r$  that varies slowing with radius, consistent with the ion and electronic temperature profiles. On the other hand and for simplicity, a constant-accretion Mach number (larger than unity) has been assumed in the JED, consistent with self-similar calculations. In a more realistic situation, we would also expect a varying accretion Mach number. However, observations require a supersonic accretion flow throughout the hot accretion flow ([Marcel & Neilsen 2021](#); [Kawamura et al. 2022](#)), which means that the accretion speed (hence the jet torque) must adapt as well. Thus, although there is a caveat in our calculations here, this should not affect the main arguments presented in this section.

It remains an open question how much of the JED volume that is located beyond the innermost region aligned with the black hole might undergo solid-body precession. We stress, however, that in order to recover the observational correlation encapsulated in Eq. (1), this volume would have to reach a radius  $r_t \equiv r_J$ , which is doubtful according to both the previous causal argument and torque estimates. In the case of high tilts leading to disk tearing at a radius  $r_t$  ([Liska et al. 2021](#)), this radius would then also have to coincide with the transition to an outer SAD accretion mode. Within our JED-SAD framework, it is unclear to us why  $r_J$ , which marks the transition from  $\mu$  near unity in the JED to  $\mu \sim 10^{-3}$  in the inner SAD, should always be coincident with the tearing radius  $r_t$ .

Finally, [Marcel & Neilsen \(2021\)](#) have reached a similar conclusion based only on observational constraints. In order to reproduce the observed X-ray spectra during the most luminous hard states, the hot flow must accrete at sonic to

supersonic speeds (see, e.g., Marcel & Neilsen 2021; Kawamura et al. 2022), which cannot be reached with typical viscous torques. Because type C QPOs are prevalent in these luminous states, the authors concluded that solid-body LT-precession is probably not the driving mechanism.

The existence of a black hole-aligned precessing inner JED region translates into an inner jet precession and might therefore contribute to produce type A and/or type B LFQPOs (Stevens & Uttley 2016; Liska et al. 2019, 2021; Kylafis et al. 2020; Ma et al. 2021). It might also provide the geometrical effect that is invoked to explain the influence of the source inclination on both the QPO amplitude and lags (e.g., Motta et al. 2015; Heil et al. 2015; van den Eijnden et al. 2017). According to the above discussion, however, we doubt that solid-body LT-precession could be the generic physical mechanism responsible for type C QPOs in all XrBs, and another mechanism therefore needs to be found (see also Nathan et al. 2022).

### 3. LFQPOs as the disk signature of a jet instability

Type C LFQPOs are detected in the hard energy band, which is associated with a corona or hot inner flow (but see the discussion in Rodriguez et al. 2004a, 2008), but their frequencies show a tight correlation with the inner standard accretion disk radius, which is the JED-SAD transition radius  $r_J$  in our view (Eq. (1)). The difficulty is reconciling this correlation with a factor  $\chi \sim 100$ , which requires a secular process.

In the JED-SAD framework, two bipolar self-confined jets are magnetically launched from the inner JED. Thus, instead of searching for a secular instability within the disk itself, we propose that these LFQPOs are the disk response to some instability that is triggered in the jets themselves, away from the disk. This idea could naturally reconcile the low frequency of type C QPOs (long-term or large-scale behavior) with their apparent link with the transition radius  $r_J$ . Several aspects must be considered: (i) How can a jet instability still impact the underlying disk? (ii) Why would it have an influence on the JED spectrum? (iii) What type of jet instability would then be necessary?

#### 3.1. Causal connection with the underlying disk

We first assume that jets launched below  $r_J$  are indeed prone to some global instability. Because jets are clearly observed up to large scales, this instability must not lead to jet disruption. We thus only require that its nonlinear stage leads to some local plasma and electric current reorganization, ending up mostly in jet wobbling. This wobbling defines a frequency that is then expected to be conveyed backward to the disk through waves. If this instability is triggered in the causally connected jet region, namely before the fast-magnetosonic (FM) surface, then FM waves can indeed propagate upstream and reach the disk (in a time of about the Keplerian orbital timescale at  $r_J$ ; e.g., Ferreira & Casse 2004) so that we expect them to lead only to some broadband noise. Far longer timescales and/or spatial scales must be at play in order to trigger type C QPOs, however.

We are thus led to assume that this jet wobbling occurs beyond the FM surface. In this case, waves can no longer propagate upstream within the jet. However, the JED-SAD framework requires the existence of a large-scale vertical field threading the whole accretion disk. Although the super-FM jet is defined with the magnetic flux threading the JED, there is still a magnetic field around it, threading the SAD. This field defines a magnetic sheath inside which the inner jet is propagating (see sketch in Fig. 1). This outer sheath being sub-FM (e.g., in the simulations

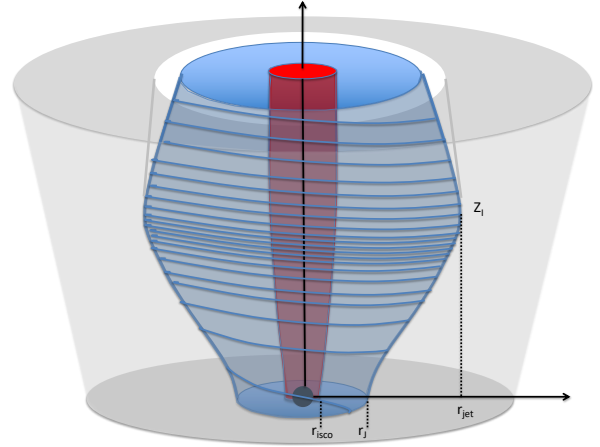


**Fig. 1.** JED-SAD hybrid disk configuration and its associated outflows in the hard state. The JED is settled from the ISCO  $r_{\text{ISCO}}$  up to the transition radius  $r_J$ , beyond which an SAD is established. A vertical large-scale magnetic field threads the whole region up to the axis. The red zone is the relativistic Blandford-Znajek spine, the blue zone is the sub-relativistic to mildly relativistic Blandford-Payne jet launched from the JED, and the gray shaded area is the outer magnetic sheath, with only an unsteady sub-Alfvénic outflow (wind). The optimal location for the jet instability is the altitude  $z_I$ , where the outer magnetic surface anchored at  $r_J$  is starting to recollimate toward the axis, defining the jet radius  $r_{\text{jet}}$ .

of Murphy et al. 2010), waves can still propagate downward and thereby reach the disk. The path followed by these waves is not straightforward as the medium is inhomogeneous and waves are known to undergo some refraction. However, we expect modes to propagate preferentially along the sheath down to the transition radius  $r_J$  (much like a surface mode). Moreover, when these waves reach the sub-FM zone of the inner jet, they will start to act as a lateral source localized at the limiting surface anchored at  $r_J$ . This in turn leads to perturbations that this time can propagate within the jet and reach the whole JED extension.

Our main assumption is therefore the existence of a jet instability that is triggered at a distance  $z_I$  and leads to subsequent jet wobbling. This lateral jet displacement bounces back on the magnetic sheath, which triggers the propagation of perturbations. How long it takes for these perturbations to reach the disk is a difficult question, as it requires following the path of these waves. However, when the instability is triggered, the perturbations in the jet itself are advected downstream, leaving behind the same physical conditions that have led to the triggering of the instability. As a consequence, it will grow again near  $z_I$  and lead to another unstable regime with a global jet displacement. As long as the conditions for the jet instability are met, we expect this cycle to continue and thereby define a jet wobbling frequency  $\nu_I$  that is mostly related to the timescale required for the lateral jet displacement. This frequency will be observed as an LFQPO in the disk.

#### 3.2. Impact on the accretion flow: LFQPOs

The jet instability acts like a hammer hitting the sheath with a characteristic frequency  $\nu_I$ . The information (wobbling frequency and released energy) is transported backward by FM waves traveling along the magnetic sheath surrounding the jet near  $r_J$ . A fraction of this energy is then expected to be spread throughout the JED through a lateral shower of FM modes triggered at the magnetic sheath near the disk. Computing how



these perturbations will affect the emitted hard X-ray spectrum and lead to an observable LFQPO requires complex radiative calculations.

The fluctuations, typically 1–20% seen in hard X-rays, can be understood through two independent processes, both related to these incoming waves. Because they are FM waves, some vertical compression of the hot JED material is naturally expected, leading to some enhanced dissipation (thus emission) at the disk surface. The second aspect is related to the possible modifications of the jet torque that acts upon the disk. These waves are indeed expected to also introduce fluctuations in the local toroidal magnetic field, hence in the torque due to the jet. As a consequence, fluctuations of the JED accretion rate and in the related release of accretion energy are expected that respond with the same quasi-periodic frequency  $\nu_I$ .

However, to obtain a proper QPO with a rather large quality factor, an almost resonant cavity is required. As shown by Cabanac et al. (2010), the JED itself may play this role and also act as a low-bandpass medium: its response to white-noise excitation is a flat-top noise power spectral density at low frequencies and a red noise at high frequency. In other words, if the jet acts like a hammer, the bell would be the JED<sup>2</sup>. A QPO is therefore expected to arise at a frequency  $\nu_I$ , the same at each energy bin and related to the dynamical (epicyclic or Keplerian) frequency at  $r_J$  (see below). It is unclear, however, how the existence of the outer magnetic sheath and intrinsic fluctuations of the dissipation within the JED will affect the calculations reported by Cabanac et al. (2010). This deserves further investigations.

### 3.3. Which instability could lead to jet wobbling?

An MHD jet is a helical magnetic structure that can be seen as an ensemble of poloidal magnetic surfaces, nested around each other and in pressure equilibrium with the surrounding medium. In our JED-SAD framework, the jet is mostly the super-FM outflow emitted by the underlying JED established between the ISCO  $r_{\text{isco}}$  and  $r_J$  (blue region in Fig. 1). Below  $r_{\text{isco}}$ , magnetic field lines are brought in and concentrated in the plunging region and black hole horizon (red region in Fig. 1), leading to the production of a relativistic tenuous spine through the Blandford-Znajek process (Blandford & Znajek 1977). It is unclear, however, whether the existence of this spine has any dynamical impact on the outer Blandford-Payne jet. Radio observations can be accounted for using only the power carried by this outer flow component (Marcel et al. 2018a, 2019, 2020). In any case, if some jet instability is to give rise to an LFQPO related to  $r_J$ , however, it must involve the distant and thus nonrelativistic jet region. We therefore neglect the effect of the spine below (but see Barnier et al. 2022).

Jets are prone to many instabilities such as pressure-driven (PD), current-driven (CD), and Kelvin-Helmholtz (KH) instabilities (plus any combination of them; Appl & Camenzind 1992; Baty & Keppens 2002, for a review, see, e.g., Hardee 2013). All these instabilities can either trigger radially localized, internal, and surface modes or long-wavelength body modes. The final nonlinear outcome of these instabilities can reach from a simple internal redistribution of jet quantities (leading to a nonlinear jet stabilization) to the production of internal shocks and/or MHD turbulence. In this latter case, a significant energy dissipation may eventually lead to a complete disruption of the jet

on a finite distance. There is no consensus on which instability would be dominant in a jet as the existence and relative strength (growth rate) of these instabilities depend on the radial stratification of the jet, which is still poorly understood.

In this paper, we envision a nondestructive instability that gives birth to a long-wavelength instability at an altitude  $z_I$ , that is, a global body-mode that involves lateral displacements of the whole outflow of radius  $r_{\text{jet}}$ . The jet radius  $r_{\text{jet}}$  is the radius achieved at the altitude  $z_I$  of the magnetic surface anchored at  $r_J$ . As discussed above, this displacement will bounce at the interface of the jet and the magnetic sheath and trigger upstreaming (toward the disk) propagations of MHD disturbances. The jet displacement itself is advected downstream of the flow and becomes potentially detectable farther out as jet wobbling. This allows another sequence (instability, jet displacement, and bouncing) to set in at  $z_I$ , so that the whole process will be quasi-periodic with a characteristic frequency  $\nu_I$ . The altitude  $z_I$  is therefore the smallest distance from the source at which this instability can take place. The frequency  $\nu_I$  is related to the timescale involved for allowing FM waves to travel across the jet radius at  $z_I$ , so that it can behave as a whole (body mode). The frequency can thus be estimated as

$$\nu_I \sim \frac{V_{\text{FM}}}{2r} \Big|_{r_{\text{jet}}}, \quad (3)$$

where  $V_{\text{FM}}$  is the FM phase speed at the jet radius  $r_{\text{jet}}$ . Assuming that the jet is cold and dominated by the toroidal magnetic field, this leads to

$$V_{\text{FM}} \simeq V_{A\phi} = \frac{B_\phi}{\sqrt{\mu_o \rho}} = \frac{m}{m^2 - 1} \left( 1 - \frac{r_A^2}{r^2} \right) \Omega_* r \simeq \frac{\Omega_* r}{m}, \quad (4)$$

evaluated at  $r = r_{\text{jet}} \gg r_J$  (Pelletier & Pudritz 1992). In this expression,  $\Omega_* \simeq \Omega_K(r_J)$  is the angular velocity of the magnetic surface (MHD invariant),  $r_A$  is the Alfvén radius at which the flow becomes super-Alfvénic, and  $m = u_p/V_{A\phi}$  is the Alfvénic Mach number, assumed to be much larger than unity.

In order for the characteristic frequency  $\nu_I$  to be identical to the LFQPO frequency  $\nu_C$ , the condition

$$m \sim \pi \chi \quad (5)$$

on the Alfvénic Mach number  $m$  must be fulfilled, where we made use of Eq. (1). This is possible as long as magnetically driven jets from accretion disks are able to reach a value  $m$  between  $\sim 220$  and 400 for  $\chi$  ranging from  $\sim 70$  to 130 (Marcel et al. 2020). This is indeed the case, as shown, for instance, in Fig. 8 in Ferreira (1997). It corresponds to tenuous MHD solutions that become super-FM (i.e.,  $n = u_p/V_{\text{FM}}$  of a few) and that expand the most, with  $r_{\text{jet}}/r_J$  reaching values of a few hundreds up to one thousand (see his Fig. 6). Equation (5) is not a fine-tuning, but instead a selection (and a property) of the underlying MHD solution established within the JED. The fact that these MHD solutions have been already computed is quite promising for our scenario.

Jets are highly inhomogeneous media, with tremendous magnetic and velocity gradients whose effects on the development of an instability are not yet fully understood (see, e.g., Bondeson et al. 1987; Birkinshaw 1991; Kersalé et al. 2000; Frank et al. 2000; Appl 1996; Mizuno et al. 2009, 2011, 2014; Kim et al. 2015, 2016, 2018). We note, however, that no instability is expected below the Alfvén surface. The stabilizing magnetic tension due to the poloidal magnetic field is too strong. In addition, just after the Alfvén point, MHD

<sup>2</sup> This is somewhat similar to the approach of Psaltis & Norman (2000): the hot inner JED acts as a filtering cavity of all incoming perturbations.



jets undergo a huge lateral expansion leading to  $|B_\phi| \gg B_p$  and  $m \gg 1$ , which drastically reduces the growth rate of any CD and KH modes, in contrast to cylindrical jet configurations (see, e.g., [Rosen & Hardee 2000](#); [Moll et al. 2008](#); [McKinney & Blandford 2009](#); [Porth & Komissarov 2015](#); [Kim et al. 2016](#)). We therefore expect the triggering of CD or KH instabilities only at an altitude  $z_I$  at which the jet radius has achieved some limiting value (i.e., a quasi-cylindrical jet), determined by the transverse equilibrium with its surrounding medium.

Our analysis highlights the capital role played by the magnetic surface anchored at  $r_J$ . This surface corresponds to the last self-confined magnetic surface and thus to a maximum of the electric current flowing inside the jet. Because a sub-FM flow (probably even sub-Alfvénic) is expected to be established in the outer magnetic sheath (the gray portion of the magnetic flux anchored beyond  $r_J$  in Fig. 1), however, a velocity shear is also necessarily present. Moreover, because the lateral equilibrium must be fulfilled, the outer (gas plus magnetic) pressure must balance the inner jet ram pressure and the magnetic deconfining force acting on the magnetic sheath. A density increase is thus to be expected in this region. These two elements (inner high-speed jet surrounded by a denser and slower outflow) are very similar to those found at the spine-jet interface and are clearly observed in GRMHD simulations. In accordance with our discussion, a CD kink instability leading to jet wobbling and wiggles is indeed seen to develop (see, e.g., [McKinney & Blandford 2009](#); [Tchekhovskoy et al. 2011](#)). In addition, the instability does not lead to jet destruction, probably because of the existence of this velocity shear ([Mizuno et al. 2014](#); [Kim et al. 2016, 2018](#)).

We argued above that the optimal location for triggering a jet instability leading to jet wobbling would be the altitude  $z_I$  at which the jet radius would reach its maximum size. This situation is expected in self-similar Blandford-Payne jets and their generalization, as these types of jets always undergo a magnetic recollimation toward the axis ([Contopoulos & Lovelace 1994](#); [Ferreira 1997](#); [Polko et al. 2010](#)). The existence of this intrinsic recollimation may cause a pressure mismatch at the jet-sheath interface (the white zone depicted in Fig. 1), leading to a possible recollimation instability ([Matsumoto & Masada 2013](#); [Matsumoto et al. 2017](#)). This new 3D instability, first associated with a Rayleigh-Taylor instability, is a variant of the centrifugal instability emerging along curved streamlines ([Gourgoulatos & Komissarov 2018a,b](#)). Whether it could lead to jet destruction and not only jet wobbling, as assumed here, remains to be fully assessed. However, it has recently been shown that it could be quenched with the presence of some external azimuthal magnetic field ([Matsumoto et al. 2021](#)).

As a final note, we remark that if we assume the recollimation point to be the locus of the jet instability, then the nonrelativistic jet solutions that fulfill all constraints (super-FM, large radius, and Eq. (5)) require a quite tiny mass loading parameter along that surface, namely a disk ejection efficiency  $\xi$ , defined as  $\dot{M}_{\text{acc}} \propto r^\xi$  in the JED, satisfying  $5 \cdot 10^{-3} < \xi < 10^{-2}$  (see Figs. 6 and 8 in [Ferreira 1997](#)). These values are consistent with jet speed estimates reported for Cygnus X-1 ([Petrucci et al. 2010](#)). This range stems from exact mathematical solutions, but more realistic ones should deviate from a strict self-similarity. Although the outermost magnetic surface of the JED should fulfill that constraint, the mass loading (or ejection index  $\xi$ ) can increase progressively toward the center.

## 4. Discussion

### 4.1. Numerical simulations

Our wobbling-jet scenario is quite generic and should therefore be observed in numerical jet simulations. However, as already pointed out, not only are the physical conditions envisioned here quite demanding, they also require full 3D simulations. This jet wobbling should not be confused with jet precession due to the black hole tilt and leading to a Bardeen-Petterson-like (probably modified by large-scale magnetic fields) alignment of the innermost disk regions ([McKinney et al. 2013](#); [Liska et al. 2019, 2021](#)). Although this precession may provide the correct physical ground for high-frequency (kHz) QPOs, it cannot explain the LFQPOs discussed here (see also [Kylafis et al. 2020](#)). Instead, we rely on a body-mode instability in the super-FM regime, involving the whole jet radius and leading to quasi-periodic variations in the jet direction.

Although the stability of two-component magnetized jets is currently under study (see, e.g., [Millas et al. 2017](#) and references therein), they usually focus on the interplay between the inner relativistic spine and the outer slower and denser flow (usually referred to as the sheath in these works). We also note that with a much simpler jet profile, kink instabilities can indeed be obtained, affecting the large-scale jet morphology and giving rise to interesting quasi-periodic radiative signatures (e.g., [Tchekhovskoy & Bromberg 2016](#); [Barniol Duran et al. 2017](#); [Dong et al. 2020](#); see also the large-scale 2D simulations of [Chatterjee et al. 2019](#), showing pinch instabilities). However, we stress that a self-confined magnetized outflow must carry its own electric poloidal current and must therefore be seen as consisting of three components that are embedded in an external medium, not just two components: the axial spine, the jet, and the outer sheath.

In our view, the role of the central spine in the whole outflow collimation remains to be assessed (see, e.g., [Barnier et al. 2022](#)). The jet corresponds here to the super-FM Blandford-Payne outflow launched from the JED. The outer sheath is built up from the unavoidable magnetic flux threading the SAD region, which is settled beyond the JED. This magnetized sheath must be understood as being part of the whole outflow because it must carry the return electric current (at the jet-sheath interface) that insulates the jet from the external medium (or cocoon). Understanding the propagation and stability properties of such stratified outflows is of great importance for accreting objects. It remains a numerical challenge, however, to address the large spatial and temporal scales involved while also accounting for the complex jet stratification imposed by the underlying hybrid disk configuration.

### 4.2. Jet disruption and JED disappearance

Super-FM jets from JEDs are expected to start wobbling at some altitude  $z_I$ , but the question is whether they would be disrupted. This is a difficult question to answer theoretically, as the nonlinear saturation could be a simple readjustment of the gradients and the smearing out of the instability. In some circumstances, for instance, a CD instability leads to the stabilization of KH modes ([Baty & Keppens 2002](#)). Based on the observation that type C LFQPOs are maintained as long as there are steady compact jets (but see the discussion in [Fender et al. 2009](#); [Fender & Gallo 2014](#)), we assumed in our simplified picture that this instability does not lead to jet disruption. This requires that the jet is able to propagate up to a distance  $L = \alpha r_{\text{jet}}$  with  $\alpha$

of a few hundreds, for instance, in a time  $T = L/u_{p,\max}$  shorter than the characteristic growth time of the instability  $\tau = \nu_I^{-1}$  (e.g., Kim et al. 2016). In this expression,  $u_{p,\max}$  is the maximum poloidal speed of the jet and is thus associated with the ISCO radius  $r_{\text{isco}}$  (for simplicity, we neglect the effect of the fast spine here). As a consequence, the instability leads to jet destruction if  $\tau < T$ , which provides the condition  $u_{p,\max}/u_p(r_j) < x/2n$ , where  $n = u_p/V_{\text{VM}}$  is the FM Mach number measured in the outer jet region. This crude estimate immediately shows that as  $r_j \rightarrow r_{\text{isco}}$ , it becomes harder to maintain stability: the thinner the jet, the more fragile and prone to destruction it becomes. This is qualitatively consistent, for instance, with the fact that as the jet radius shrinks, the turbulent boundary layer due to a KH surface mode becomes on the order of the jet radius, leading thereby to its disruption (Baty & Keppens 2006; Kim et al. 2016). We thus expect a nondestructive jet wobbling whenever  $r_j \gg r_{\text{isco}}$ .

Conversely, as the JED shrinks (hard-to-soft transition), the resulting jet would become too narrow to survive the instability. This would be coincident with a dramatic jet restructuring until its complete disruption and disappearance (assumed to occur at the jet line). However, before the jet completely disappears, reconnecting events of the magnetic structure are expected to lead to the dramatic release of jet energy, possibly associated with discrete ejecta and subsequent radio flares (Homan et al. 2020; Wood et al. 2021).

This evidence of a link between the appearance of type B QPOs and the launch of discrete ejecta fits quite well within our jet instability scenario for QPOs. As  $r_j \rightarrow r_{\text{isco}}$ , we also expect the jet to become narrower due to the (relatively stronger) external magnetic pressure (Spruit et al. 1997). This translates into a QPO frequency  $\nu_I \sim \Omega_K(r_j)/(2m)$  (Eq. (3)) that could change while the transition radius  $r_j$  remains almost constant. A smaller opening of the magnetic field lines leads to a smaller jet acceleration, hence to a smaller Alfvénic Mach number  $m$ . As a consequence, the QPO frequency may (slightly) increase, while there is no detectable change in the inner cold disk radius (Kara et al. 2019; Ma et al. 2021). This aspect of jet collimation has not been fully investigated so far.

#### 4.3. Detectable signatures: IR QPOs and jet wobbling

Within the framework of wobbling jets, it appears to be rather natural to have QPOs at the same frequency and at energy bands usually associated with jet emission (i.e., OIR). The jet instability is triggered at an altitude  $z_I$  (the recollimation zone) and gives rise to perturbations that propagate both up- and downstream. It takes a time  $\Delta t_X$  for the upstream waves to travel down to the disk and give rise to an observable QPO in the X-ray band. Because jet wobbling is quasi-periodically produced, however, it may well give rise to an OIR QPO at a distance  $z_{\text{IR}} > z_I$  after a time  $\Delta t_{\text{IR}} \sim (z_{\text{IR}} - z_I)/u_p$ , where  $u_p$  is the flow speed (and possibly to some variability signature in radio bands; Tetarenko et al. 2019). There is therefore no obvious reason why  $\Delta t_X$  should always be shorter than  $\Delta t_{\text{IR}}$ , so that we do not expect any clear trend for the time lag between X and OIR QPOs (see also Veledina et al. 2013, 2015).

This is consistent with OIR QPOs lagging behind X-ray QPOs with  $\sim 0.1$  s in several XrBs (Gandhi et al. 2010, 2017; Kalamkar et al. 2016), but also with the nondetection of any lag in MAXI J1535-571 (Vincentelli et al. 2021) or even X-rays possibly lagging behind the optical QPO in MAXI J1820+070 (Paice et al. 2021). Moreover, there is evidence of different properties between the two QPOs, such as the rms-flux relation (Vincentelli et al. 2018) or the time evolution of

the power spectral density (Vincentelli et al. 2019). Although a common origin for X and OIR QPOs is quite natural within our framework, it seems plausible that some filtering effect occurs as perturbations are propagating downstream the jet (see also Hynes et al. 2003).

It may be quite hard to probe jet wobbling in black hole XrB jets because of the lack of resolution (but see Miller-Jones et al. 2019). In the context of AGN, this instead requires a long-term monitoring of jets. It is well known that AGN jets display nonradial motions that are indicative of accelerated, nonballistic motions (see, e.g., Lister et al. 2016; Boccardi et al. 2017). Jet wobbling has been inferred in various BL Lac sources, however, implying timescales from 2 to 20 yr (e.g., Agudo et al. 2012; Arshakian et al. 2020 and references therein). Walker et al. (2018) have also found evidence of such a pattern in the radio galaxy M87, with a period of  $\sim 9$  yr. When scaled down to a 10 solar mass black hole, this value provides a frequency around 2 Hz, which is consistent with the range of LFQPOs in black hole XrBs.

In the realm of young stellar objects, the situation is quite similar. Protostellar jets seen in the optical are thought to arise from the innermost disk regions, where orbital periods range from a few days to about a year (Ferreira et al. 2006a; Ray et al. 2007 and references therein). On the other hand, these jets harbor knots that resemble bow shocks whose separations are indicative of timescales ranging from years to tens of years (e.g., López-Martín et al. 2003; Agra-Amboage et al. 2011; Ellerbroek et al. 2014; Lee et al. 2017; Tabone et al. 2017). These timescales are too short to be explained by perturbations due to a companion star, and they are too long to be related to any dynamical timescale at the launching radius (see, e.g., jet wobbling in HH30; Louvet et al. 2018 and references therein). Instead of relating these knots to time-variable ejection events from the source, we propose to relate them to the same jet instability. This instability could be very similar to the one invoked here to explain LFQPOs around compact objects, although it might lead to jet disruption with a subsequent ballistic motion in some sources.

## 5. Conclusion

Building upon the success of the JED-SAD framework to reproduce the radio emission and X-rays spectral energy distributions during various cycles of the archetypal source GX 339-4, we addressed the question of the origin of type C LFQPOs. We first critically analyzed the most common models invoked for these QPOs: (1) models searching for a specific process triggered at the transition radius  $r_j$ , (2) the accretion-ejection instability, and (3) the solid-body Lense-Thirring disk precession model. We showed that the first two types of models face major theoretical issues that are so far unsolved, and that the published versions of these models do not account for the observed tight correlation with the disk transition radius (Eq. (1)). We also argued that these models cannot be operating within the JED-SAD framework.

We then discussed the case of the solid-body LT-precession model, which is invoked whenever the black hole spin is misaligned with the disk angular momentum vector. We argued that evidence in GRMHD simulations for this solid-body behavior were not fully convincing, especially in the case of highly magnetized accretion flows. This therefore casts doubt on the capability of this model to operate within the JED-SAD framework (at least for moderate black hole tilts). As suggested by current numerical simulations, however, the innermost JED region, up to a few  $r_g$ , would probably be aligned with the black hole spin,

leading to an inner jet precession (i.e., a precession of both the Blandford-Znajek axial spine and the innermost zones of the surrounding Blandford-Payne jet). Whether some fraction of the JED that is located beyond the aligned region would undergo solid-body LT-precession remains an open issue, however, that deserves further numerical simulations that are long enough and tailored to maintain an outer cold thin disk. We argued, however, that such an effect would hardly be efficient up to the transition radius  $r_J$  with the outer SAD, as required by observations.

We propose instead that the JED-SAD framework offers the conditions allowing for a jet wobbling, namely a nondestructive long-wavelength 3D body mode probably triggered by a kink or recollimation instability in the super-FM jet regime. This wobbling, triggered away from the disk, will nevertheless affect the disk through FM waves traveling upstream along the surrounding magnetic sheath, as well as downstream the jet. This outer magnetic sheath is the key ingredient allowing us to connect the fast inner jet, which hammers quasi-periodically against the sheath, to the underlying resonant disk (JED). This scenario offers a unique explanation for the existence of QPOs seen in disk (X-rays) and jet (UV and OIR) emission signatures.

The theoretical foundations of this scenario are threefold: (i) existence of exact calculations of MHD accretion-ejection flows with the correct required properties, (ii) self-consistent thermal disk balance calculations, with thorough comparisons to observations, and (iii) current knowledge about MHD instabilities in stratified super-FM flows. Notwithstanding these facts and hints, the proposed dynamical mechanism as well as its radiative consequences remain to be firmly established. To do this, global 3D jet simulations must be designed so that such an instability could indeed be observed, with its upstreaming perturbations heading toward the disk. On the radiative side, the work of Cabanac et al. (2010) should be extended in order to incorporate the existence of these incoming perturbations, and possibly also address the question of the time lags and their energy dependence.

We finally note that polarization measurements by IXPE, just launched in December 2021, or if it is selected, and in a more distant future, by eXTP, may bring great insight into LFQPOs. If swings in polarization angle were detected, it would provide stringent conditions that all the models and scenarios discussed above will have to explain. This is provided that these constraints are usable, as required integration times are much longer than the periods that are probed (but see, e.g., Ingram & Maccarone 2017).

*Acknowledgements.* J.F. would like to thank Adam Ingram and Matthew Liska, as well as the referee, Chris Done, for interesting discussions that allowed to improve the quality of the paper. We acknowledge financial support from the CNES French space agency and PNHE program of French CNRS.

## References

- Abramowicz, M. A., Igumenshchev, I. V., & Lasota, J.-P. 1998, *MNRAS*, 293, 443
- Agra-Amboage, V., Dougados, C., Cabrit, S., & Reunanen, J. 2011, *A&A*, 532, A59
- Agudo, I., Marscher, A. P., Jorstad, S. G., et al. 2012, *ApJ*, 747, 63
- Appl, S. 1996, *A&A*, 314, 995
- Appl, S., & Camenzind, M. 1992, *A&A*, 256, 354
- Arshakian, T. G., Pushkarev, A. B., Lister, M. L., & Savolainen, T. 2020, *A&A*, 640, A62
- Avara, M. J., McKinney, J. C., & Reynolds, C. S. 2016, *MNRAS*, 462, 636
- Balbus, S. A. 2003, *ARA&A*, 41, 555
- Balbus, S. A., & Hawley, J. F. 1991, *ApJ*, 376, 214
- Bardeen, J. M., & Petterson, J. A. 1975, *ApJ*, 195, L65
- Barnier, S., Petrucci, P. O., Ferreira, J., et al. 2022, *A&A*, 657, A11
- Barniol Duran, R., Tchekhovskoy, A., & Giannios, D. 2017, *MNRAS*, 469, 4957
- Baty, H., & Keppens, R. 2002, *ApJ*, 580, 800
- Baty, H., & Keppens, R. 2006, *A&A*, 447, 9
- Begelman, M. C., & Armitage, P. J. 2014, *ApJ*, 782, L18
- Belloni, T., Homan, J., Casella, P., et al. 2005, *A&A*, 440, 207
- Birkinkshaw, M. 1991, *MNRAS*, 252, 505
- Blandford, R. D., & Payne, D. G. 1982, *MNRAS*, 199, 883
- Blandford, R. D., & Znajek, R. L. 1977, *MNRAS*, 179, 433
- Boccardi, B., Krichbaum, T. P., Ros, E., & Zensus, J. A. 2017, *A&ARv*, 25, 4
- Bondeson, A., Iacono, R., & Bhattacharjee, A. 1987, *Phys. Fluids*, 30, 2167
- Cabanac, C., Henri, G., Petrucci, P., et al. 2010, *MNRAS*, 404, 738
- Casella, P., Belloni, T., Homan, J., & Stella, L. 2004, *A&A*, 426, 587
- Chatterjee, K., Liska, M., Tchekhovskoy, A., & Markoff, S. B. 2019, *MNRAS*, 490, 2200
- Chatterjee, K., Younsi, Z., Liska, M., et al. 2020, *MNRAS*, 499, 362
- Contopoulos, J., & Lovelace, R. V. E. 1994, *ApJ*, 429, 139
- Corbel, S., Fender, R. P., Tzioumis, A. K., et al. 2000, *A&A*, 359, 251
- Corbel, S., Nowak, M. A., Fender, R. P., Tzioumis, A. K., & Markoff, S. 2003, *A&A*, 400, 1007
- Corbel, S., Coriat, M., Brocksopp, C., et al. 2013, *MNRAS*, 428, 2500
- de Ruiter, I., van den Eijnden, J., Ingram, A., & Uttley, P. 2019, *MNRAS*, 485, 3834
- Done, C., Gierliński, M., & Kubota, A. 2007, *A&ARv*, 15, 1
- Dong, L., Zhang, H., & Giannios, D. 2020, *MNRAS*, 494, 1817
- Dunn, R. J. H., Fender, R. P., Körding, E. G., Belloni, T., & Cabanac, C. 2010, *MNRAS*, 403, 61
- Dyda, S., & Reynolds, C. S. 2020, ArXiv e-prints [arXiv:2008.12381]
- Ellerbroek, L. E., Podio, L., Dougados, C., et al. 2014, *A&A*, 563, A87
- Esin, A. A., McClintock, J. E., & Narayan, R. 1997, *ApJ*, 489, 865
- Falcke, H., Körding, E., & Markoff, S. 2004, *A&A*, 414, 895
- Fender, R., & Gallo, E. 2014, *Space Sci. Rev.*, 183, 323
- Fender, R. P., Belloni, T. M., & Gallo, E. 2004, *MNRAS*, 355, 1105
- Fender, R. P., Homan, J., & Belloni, T. M. 2009, *MNRAS*, 396, 1370
- Ferreira, J. 1997, *A&A*, 319, 340
- Ferreira, J., & Casse, F. 2004, *ApJ*, 601, L139
- Ferreira, J., & Pelletier, G. 1995, *A&A*, 295, 807
- Ferreira, J., Petrucci, P.-O., Henri, G., Saugé, L., & Pelletier, G. 2006a, *A&A*, 447, 813
- Ferreira, J., Dougados, C., & Cabrit, S. 2006b, *A&A*, 453, 785
- Fragile, P. C. 2009, *ApJ*, 706, L246
- Fragile, P. C., & Anninos, P. 2005, *ApJ*, 623, 347
- Fragile, P. C., Blaes, O. M., Anninos, P., & Salmonson, J. D. 2007, *ApJ*, 668, 417
- Frank, A., Lery, T., Gardiner, T. A., Jones, T. W., & Ryu, D. 2000, *ApJ*, 540, 342
- Gallo, E., Fender, R. P., & Pooley, G. G. 2003, *MNRAS*, 344, 60
- Gandhi, P., Dhillon, V. S., Durant, M., et al. 2010, *MNRAS*, 407, 2166
- Gandhi, P., Bachetti, M., Dhillon, V. S., et al. 2017, *Nat. Astron.*, 1, 859
- Gourgouliatos, K. N., & Komissarov, S. S. 2018a, *Nat. Astron.*, 2, 167
- Gourgouliatos, K. N., & Komissarov, S. S. 2018b, *MNRAS*, 475, L125
- Hardee, P. E. 2013, in *The Innermost Regions of Relativistic Jets and Their Magnetic Fields*, ed. J. L. Gómez, *Eur. Phys. J. Web Conf.*, 61
- Heil, L. M., Uttley, P., & Klein-Wolt, M. 2015, *MNRAS*, 448, 3348
- Homan, J., Bright, J., Motta, S. E., et al. 2020, *ApJ*, 891, L29
- Hynes, R. I., Haswell, C. A., Cui, W., et al. 2003, *MNRAS*, 345, 292
- Ichimaru, S. 1977, *ApJ*, 214, 840
- Igumenshchev, I. V., Narayan, R., & Abramowicz, M. A. 2003, *ApJ*, 592, 1042
- Ingram, A. R., & Maccarone, T. J. 2017, *MNRAS*, 471, 4206
- Ingram, A. R., & Motta, S. E. 2019, *New Astron. Rev.*, 85, 101524
- Ingram, A., Done, C., & Fragile, P. C. 2009, *MNRAS*, 397, L101
- Jacquemin-Ide, J., Lesur, G., & Ferreira, J. 2021, *A&A*, 647, A192
- Kalamkar, M., Casella, P., Uttley, P., et al. 2016, *MNRAS*, 460, 3284
- Kara, E., Steiner, J. F., Fabian, A. C., et al. 2019, *Nature*, 565, 198
- Kato, S., & Manmoto, T. 2000, *ApJ*, 541, 889
- Kawamura, T., Axelsson, M., Done, C., & Takahashi, T. 2022, *MNRAS*, 511, 536
- Kersalé, E., Longaretti, P. Y., & Pelletier, G. 2000, *A&A*, 363, 1166
- Kim, J., Balsara, D. S., Lyutikov, M., et al. 2015, *MNRAS*, 450, 982
- Kim, J., Balsara, D. S., Lyutikov, M., & Komissarov, S. S. 2016, *MNRAS*, 461, 728
- Kim, J., Balsara, D. S., Lyutikov, M., & Komissarov, S. S. 2018, *MNRAS*, 474, 3954
- Krolik, J. H., & Hawley, J. F. 2015, *ApJ*, 806, 141
- Kubota, A., Ebisawa, K., Makishima, K., & Nakazawa, K. 2005, *ApJ*, 631, 1062
- Kylafis, N. D., & Belloni, T. M. 2015, *A&A*, 574, A133
- Kylafis, N. D., Reig, P., & Papadakis, I. 2020, *A&A*, 640, L16
- Lee, C.-F., Ho, P. T. P., Li, Z.-Y., et al. 2017, *Nat. Astron.*, 1, 0152
- Liska, M., Hesp, C., Tchekhovskoy, A., et al. 2018, *MNRAS*, 474, L81
- Liska, M., Tchekhovskoy, A., Ingram, A., & van der Klis, M. 2019, *MNRAS*, 487, 550



- Liska, M., Tchekhovskoy, A., & Quataert, E. 2020, *MNRAS*, 494, 3656
- Liska, M., Hesp, C., Tchekhovskoy, A., et al. 2021, *MNRAS*, 507, 983
- Lister, M. L., Aller, M. F., Aller, H. D., et al. 2016, *AJ*, 152, 12
- López-Martín, L., Cabrit, S., & Dougados, C. 2003, *A&A*, 405, L1
- Louvet, F., Dougados, C., Cabrit, S., et al. 2018, *A&A*, 618, A120
- Lubow, S. H., Ogilvie, G. I., & Pringle, J. E. 2002, *MNRAS*, 337, 706
- Ma, X., Tao, L., Zhang, S.-N., et al. 2021, *Nat. Astron.*, 5, 94
- Marcel, G., & Neilsen, J. 2021, *ApJ*, 906, 106
- Marcel, G., Ferreira, J., Petrucci, P.-O., et al. 2018a, *A&A*, 617, A46
- Marcel, G., Ferreira, J., Petrucci, P.-O., et al. 2018b, *A&A*, 615, A57
- Marcel, G., Ferreira, J., Clavel, M., et al. 2019, *A&A*, 626, A115
- Marcel, G., Cangemi, F., Rodriguez, J., et al. 2020, *A&A*, 640, A18
- Marcel, G., Ferreira, J., Petrucci, P. O., et al. 2022, *A&A*, 659, A194
- Marino, A., Barnier, S., Petrucci, P.-O., et al. 2021, *A&A*, 656, A63
- Markwardt, C. B., Swank, J. H., & Taam, R. E. 1999, *ApJ*, 513, L37
- Marshall, M. D., Avara, M. J., & McKinney, J. C. 2018, *MNRAS*, 478, 1837
- Matsumoto, J., & Masada, Y. 2013, *ApJ*, 772, L1
- Matsumoto, J., Aloy, M. A., & Perucho, M. 2017, *MNRAS*, 472, 1421
- Matsumoto, J., Komissarov, S. S., & Gourgouliatos, K. N. 2021, *MNRAS*, 503, 4918
- McKinney, J. C., & Blandford, R. D. 2009, *MNRAS*, 394, L126
- McKinney, J. C., Tchekhovskoy, A., & Blandford, R. D. 2012, *MNRAS*, 423, 3083
- McKinney, J. C., Tchekhovskoy, A., & Blandford, R. D. 2013, *Science*, 339, 49
- Merloni, A., Heinz, S., & di Matteo, T. 2003, *MNRAS*, 345, 1057
- Meyer-Hofmeister, E., Liu, B. F., & Meyer, F. 2005, *A&A*, 432, 181
- Millas, D., Keppens, R., & Meliani, Z. 2017, *MNRAS*, 470, 592
- Miller-Jones, J. C. A., Tetarenko, A. J., Sivakoff, G. R., et al. 2019, *Nature*, 569, 374
- Mineshige, S., Hirano, A., Kitamoto, S., Yamada, T. T., & Fukue, J. 1994, *ApJ*, 426, 308
- Mizuno, Y., Lyubarsky, Y., Nishikawa, K.-I., & Hardee, P. E. 2009, *ApJ*, 700, 684
- Mizuno, Y., Hardee, P. E., & Nishikawa, K.-I. 2011, *ApJ*, 734, 19
- Mizuno, Y., Hardee, P. E., & Nishikawa, K.-I. 2014, *ApJ*, 784, 167
- Moll, R., Spruit, H. C., & Obergaulinger, M. 2008, *A&A*, 492, 621
- Motta, S. E. 2016, *Astron. Nachr.*, 337, 398
- Motta, S. E., Casella, P., Henze, M., et al. 2015, *MNRAS*, 447, 2059
- Muno, M. P., Morgan, E. H., & Remillard, R. A. 1999, *ApJ*, 527, 321
- Murphy, G. C., Ferreira, J., & Zanni, C. 2010, *A&A*, 512, A82
- Narayan, R., & Yi, I. 1994, *ApJ*, 428, L13
- Narayan, R., Igumenshchev, I. V., & Abramowicz, M. A. 2003, *PASJ*, 55, L69
- Nathan, E., Ingram, A., Homan, J., et al. 2022, *MNRAS*, 511, 255
- Paice, J. A., Gandhi, P., Shahbaz, T., et al. 2021, *MNRAS*, 505, 3452
- Papaloizou, J. C. B., & Lin, D. N. C. 1995, *ApJ*, 438, 841
- Pelletier, G., & Pudritz, R. E. 1992, *ApJ*, 394, 117
- Petrucci, P.-O., Ferreira, J., Henri, G., & Pelletier, G. 2008, *MNRAS*, 385, L88
- Petrucci, P. O., Ferreira, J., Henri, G., Malzac, J., & Foellmi, C. 2010, *A&A*, 522, A38
- Polko, P., Meier, D. L., & Markoff, S. 2010, *ApJ*, 723, 1343
- Porth, O., & Komissarov, S. S. 2015, *MNRAS*, 452, 1089
- Psaltis, D., & Norman, C. 2000, ArXiv e-prints [arXiv:astro-ph/0001391]
- Ray, T., Dougados, C., Bacciotti, F., Eisloffel, J., & Chrysostomou, A. 2007, in *Protostars and Planets V*, eds. B. Reipurth, D. Jewitt, & K. Keil, 231
- Remillard, R. A., & McClintock, J. E. 2006, *ARA&A*, 44, 49
- Remillard, R. A., Morgan, E. H., McClintock, J. E., Bailyn, C. D., & Orosz, J. A. 1999, *ApJ*, 522, 397
- Rodriguez, J., Varnière, P., Tagger, M., & Durouchoux, P. 2002, *A&A*, 387, 487
- Rodriguez, J., Corbel, S., Kalemci, E., Tomsick, J. A., & Tagger, M. 2004a, *ApJ*, 612, 1018
- Rodriguez, J., Corbel, S., Hannikainen, D. C., et al. 2004b, *ApJ*, 615, 416
- Rodriguez, J., Hannikainen, D. C., Shaw, S. E., et al. 2008, *ApJ*, 675, 1436
- Rosen, A., & Hardee, P. E. 2000, *ApJ*, 542, 750
- Russell, T. D., Tetarenko, A. J., Miller-Jones, J. C. A., et al. 2019, *ApJ*, 883, 198
- Salvesen, G., Simon, J. B., Armitage, P. J., & Begelman, M. C. 2016, *MNRAS*, 457, 857
- Scepi, N., Dubus, G., & Lesur, G. 2019, *A&A*, 626, A116
- Shakura, N. I., & Sunyaev, R. A. 1973, *A&A*, 24, 337
- Sobczak, G. J., McClintock, J. E., Remillard, R. A., et al. 2000, *ApJ*, 544, 993
- Sorathia, K. A., Krolik, J. H., & Hawley, J. F. 2013, *ApJ*, 777, 21
- Spruit, H. C., Foglizzo, T., & Stehle, R. 1997, *MNRAS*, 288, 333
- Stella, L., & Vietri, M. 1998, *ApJ*, 492, L59
- Stella, L., Vietri, M., & Morsink, S. M. 1999, *ApJ*, 524, L63
- Stevens, A. L., & Uttley, P. 2016, *MNRAS*, 460, 2796
- Tabone, B., Cabrit, S., Bianchi, E., et al. 2017, *A&A*, 607, L6
- Tagger, M., & Pellat, R. 1999, *A&A*, 349, 1003
- Tchekhovskoy, A., & Bromberg, O. 2016, *MNRAS*, 461, L46
- Tchekhovskoy, A., Narayan, R., & McKinney, J. C. 2011, *MNRAS*, 418, L79
- Tetarenko, A. J., Casella, P., Miller-Jones, J. C. A., et al. 2019, *MNRAS*, 484, 2987
- Ursini, F., Petrucci, P. O., Bianchi, S., et al. 2020, *A&A*, 634, A92
- van den Eijnden, J., Ingram, A., Uttley, P., et al. 2017, *MNRAS*, 464, 2643
- Varnière, P., Rodriguez, J., & Tagger, M. 2002, *A&A*, 387, 497
- Varnière, P., Tagger, M., & Rodriguez, J. 2012, *A&A*, 545, A40
- Veledina, A., Poutanen, J., & Ingram, A. 2013, *ApJ*, 778, 165
- Veledina, A., Revnivtsev, M. G., Durant, M., Gandhi, P., & Poutanen, J. 2015, *MNRAS*, 454, 2855
- Vignarca, F., Migliari, S., Belloni, T., Psaltis, D., & van der Klis, M. 2003, *A&A*, 397, 729
- Vincentelli, F. M., Casella, P., Maccarone, T. J., et al. 2018, *MNRAS*, 477, 4524
- Vincentelli, F. M., Casella, P., Petrucci, P., et al. 2019, *ApJ*, 887, L19
- Vincentelli, F. M., Casella, P., Russell, D. M., et al. 2021, *MNRAS*, 503, 614
- Walker, R. C., Hardee, P. E., Davies, F. B., Ly, C., & Junor, W. 2018, *ApJ*, 855, 128
- Wood, C. M., Miller-Jones, J. C. A., Homan, J., et al. 2021, *MNRAS*, 505, 3393
- Yuan, F., & Narayan, R. 2014, *ARA&A*, 52, 529
- Yuan, F., Cui, W., & Narayan, R. 2005, *ApJ*, 620, 905
- Zhang, L., Méndez, M., Altamirano, D., et al. 2020, *MNRAS*, 494, 1375
- Zhu, Z., & Stone, J. M. 2018, *ApJ*, 857, 34